

## LETTERS

# Lgl, Pins and aPKC regulate neuroblast self-renewal versus differentiation

Cheng-Yu Lee<sup>1</sup>, Kristin J. Robinson<sup>1</sup> & Chris Q. Doe<sup>1</sup>

How a cell chooses to proliferate or to differentiate is an important issue in stem cell and cancer biology. *Drosophila* neuroblasts undergo self-renewal with every cell division, producing another neuroblast and a differentiating daughter cell, but the mechanisms controlling the self-renewal/differentiation decision are poorly understood. Here we tested whether cell polarity genes, known to regulate embryonic neuroblast asymmetric cell division<sup>1</sup>, also regulate neuroblast self-renewal. Clonal analysis in larval brains showed that *pins* mutant neuroblasts rapidly fail to self-renew, whereas *lethal giant larvae (lgl)* mutant neuroblasts generate multiple neuroblasts. Notably, *lgl pins* double mutant neuroblasts all divide symmetrically to self-renew, filling the brain with neuroblasts at the expense of neurons. The *lgl pins* neuroblasts show ectopic cortical localization of atypical protein kinase C (aPKC), and a decrease in aPKC expression reduces neuroblast numbers, suggesting that aPKC promotes neuroblast self-renewal. In support of this hypothesis, neuroblast-specific overexpression of membrane-targeted aPKC, but not a kinase-dead version, induces ectopic neuroblast self-renewal. We conclude that cortical aPKC kinase activity is a potent inducer of neuroblast self-renewal.

*Drosophila* neuroblasts are an excellent model system in which to investigate the molecular control of self-renewal versus differentiation. Larval neuroblasts repeatedly divide asymmetrically to

self-renew a neuroblast and to produce a smaller daughter cell, called a ganglion mother cell (GMC), that typically makes two postmitotic neurons; this process enables a single neuroblast to generate many hundreds of neurons (Fig. 1a). We define self-renewal as the capacity of a neuroblast to maintain all attributes of its cell type (molecular markers and proliferation potential). In this regard, a neuroblast is very similar to a germline stem cell: both maintain their stem cell identity while generating differentiating progeny<sup>2</sup>. About 100 neuroblasts per brain lobe are formed during embryogenesis, where they proliferate briefly before entering quiescence<sup>3</sup>. Brain neuroblasts re-enter the cell cycle between 10 and 72 h after larval hatching (ALH)<sup>4</sup>, and then a stable population of ~100 mitotic, self-renewing neuroblasts is maintained (Fig. 1b). We are using this invariant neuroblast number to screen for mutants altering self-renewal versus differentiation: mutants in which a neuroblast makes two neuroblast progeny (ectopic self-renewal) will have >100 neuroblasts, whereas mutants in which a neuroblast makes two GMC progeny (failure in self-renewal) will have <100 neuroblasts. Here we have used this assay to test known cell polarity mutants for a role in neuroblast self-renewal; the results of larger genetic screens will be described elsewhere.

We assayed two classes of cell polarity regulators for an effect on larval neuroblast self-renewal. We first examined *lgl* and *discs large (dlg)* zygotic mutants, because these mutants form brain tumours<sup>5</sup>

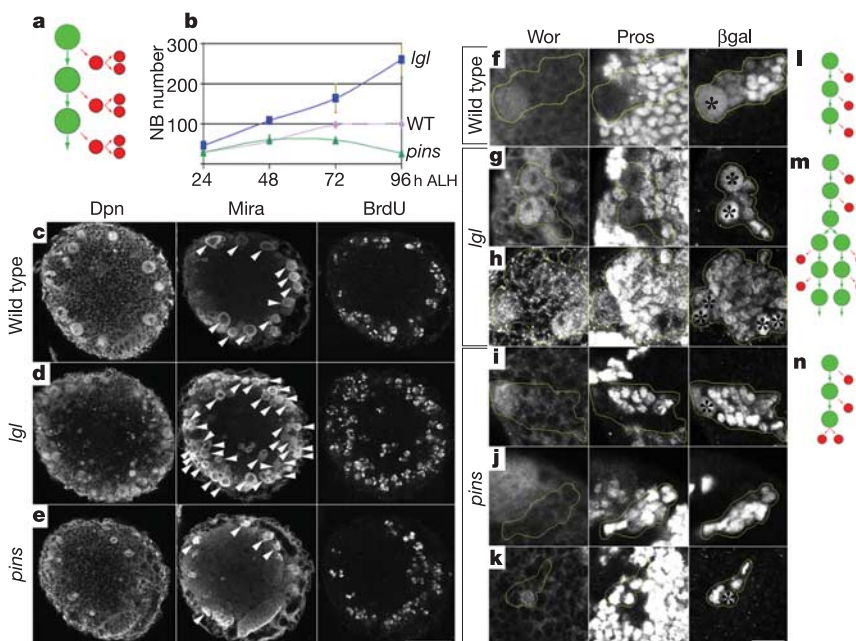


**Figure 1 | *lgl* and *pins* regulate larval neuroblast self-renewal.**

**a**, Wild-type neuroblast lineage. Green indicates neuroblast self-renewal, red indicates GMC differentiation. **b**, Quantification of neuroblast numbers from 24 to 96 h after larval hatching (ALH) ( $n = 50$  per time point per genotype). **c–e**, Single focal plane through wild-type (**c**), *lgl*<sup>33/4</sup> (**d**) and *pins*<sup>62</sup> (**e**) brains at 96 h ALH stained with the indicated markers (neuroblasts are indicated in one panel with arrowheads). **f–k**, Clonal analysis of single neuroblast lineages. Single neuroblast clones marked with  $\beta$ -galactosidase are circled; asterisks indicate neuroblasts. **f**, In wild type, neuroblast clones always contain a single *Worniu*<sup>+</sup> neuroblast and several *Prospero*<sup>+</sup> progeny (not all are shown). **g, h**, In *lgl*<sup>33/4</sup> mutants, neuroblast clones typically show two neuroblasts (**g**) or as many as six neuroblasts (**h**; only four are in the focal plane). **i–k**, In *pins*<sup>62</sup> mutants, neuroblast clones either have one (**i**) or zero (**j**) neuroblasts; in one clone, we observed a cell with both neuroblast and GMC markers (**k**). **l–m**, Interpretation of wild type and mutant lineages. Scale bars, 50  $\mu$ m (**c–e**); 10  $\mu$ m (**f–k**).

<sup>1</sup>Institutes of Neuroscience and Molecular Biology, Howard Hughes Medical Institute, University of Oregon 1254, Eugene, Oregon 97403, USA.

and promote basal protein targeting in embryonic and larval neuroblasts<sup>6–8</sup>. *Lgl* and *Dlg* have several protein interaction motifs and are localized around the neuroblast cortex<sup>6–10</sup>. In addition, we examined *pins* and *Gai* zygotic mutants; these genes regulate cell polarity in embryonic neuroblasts<sup>1</sup>, but have not been well characterized in larval neuroblasts. *Pins* and *Gai* are colocalized with Inscutable and the evolutionarily conserved Bazooka–Par6–aPKC proteins at the apical cortex of mitotic neuroblasts, and all of these proteins are partitioned into the neuroblast during cytokinesis<sup>1</sup>.

In wild-type larvae, a population of ~100 neuroblasts could be identified by the markers *Worniu*, *Deadpan* and *Miranda*, and by labelling with a pulse of 5-bromodeoxyuridine (BrdU); by contrast, the thousands of differentiating GMCs and neurons rapidly down-regulated neuroblast markers and expressed nuclear Prospero and/or *Elav* (Fig. 1b, c, and Supplementary Fig. 1a and Movie 1). We observed a clear increase in neuroblast number in *lgl* and *dlg* mutants; there were supernumerary neuroblasts at all stages examined, and all extra neuroblasts expressed *Deadpan* and *Miranda* and were proliferative on the basis of their ability to incorporate BrdU (Fig. 1b, d, Supplementary Fig. 1 and Movie 2, and data not shown). *Gai* zygotic mutants had a complex phenotype that will be described elsewhere; however, *pins* zygotic mutants showed a marked decrease in neuroblast number (Fig. 1b, e, and Supplementary Fig. 1 and Movie 3). Notably, this phenotype was not due to a subset of neuroblasts remaining quiescent, because neuroblast numbers peaked and then declined over time (Fig. 1b), and it was not due to neuroblast cell death (see below). The relatively late onset of the *pins* phenotype was probably due to the gradual depletion of maternal *pins* gene product in these larvae (C.-Y.L. and C.Q.D., unpublished data).

To determine whether the *pins* and *lgl* larval brain phenotypes were due to defects in neuroblast self-renewal, we induced positively marked genetic clones<sup>11</sup> in single neuroblasts to trace their progeny (Fig. 1f–k). We adjusted clone induction parameters to ensure that each clone was derived from a single neuroblast (1.2 clones per lobe;  $n = 20$ ). In wild-type brains, neuroblast clones always contained a single *Worniu*<sup>+</sup> *Miranda*<sup>+</sup> nuclear-Prospero<sup>-</sup> neuroblast and numerous smaller *Worniu*<sup>-</sup> *Miranda*<sup>-</sup> nuclear-Prospero<sup>+</sup> progeny (Fig. 1f;  $n = 35$  clones), confirming that wild-type neuroblasts always divide to self-renew and to generate a smaller differentiating GMC (Fig. 1l). By contrast, *lgl* mutant brains had an average of 2.3 neuroblasts per clone, with up to six neuroblasts per clone (Fig. 1g, h;  $n = 22$  clones), showing that *lgl* mutant neuroblasts can divide symmetrically to yield two neuroblasts (Fig. 1m). The opposite phenotype was seen in *pins* mutant brains: 72.8% of the clones had no neuroblast and the remainder had a single neuroblast (Fig. 1i–k;  $n = 34$  clones). The neuroblasts did not die in the *pins* mutants as the cell death marker caspase-3 was not upregulated (Supplementary Fig. 2), as neuroblast-specific expression of the p35 cell death inhibitor did not rescue the missing neuroblasts (data not shown), and as we observed one clone in which the largest cell coexpressed neuroblast and GMC markers, consistent with an intermediate stage in neuroblast-to-GMC differentiation (Fig. 1k). We conclude that wild-type neuroblasts exclusively generate neuroblast/GMC siblings; *lgl* mutant neuroblasts occasionally undergo ectopic self-renewal to generate neuroblast/neuroblast siblings; and *pins* mutant neuroblasts occasionally fail to self-renew, resulting in GMC/GMC siblings and termination of the lineage.

We next examined whether *lgl pins* double mutants had fewer neuroblasts (like *pins* mutants) or extra neuroblasts (like *lgl* mutants). Unexpectedly, we detected a phenotype in which the larval brain was full of cells expressing the neuroblast markers *Worniu*, *Miranda* and *Deadpan* and lacking expression of the neuronal marker *Elav* (Fig. 2b and Supplementary Movie 4). We assayed additional markers that distinguish neuroblasts and GMCs to determine whether these cells were neuroblasts or a hybrid neuroblast/GMC identity. We found that both wild-type neuroblasts and *lgl pins* cells actively transcribed the *worniu*, *deadpan*, *miranda* and *prospero*

genes, maintained proliferation, did not express the *Elav* neuronal differentiation marker, and did not extend axons (Fig. 2b and Supplementary Fig. 3). The only potential GMC attribute found in *lgl pins* neuroblasts was nuclear Prospero protein (data not shown) but, because wild-type neuroblasts and GMCs both contain Prospero protein, which can accumulate in neuroblast nuclei if not properly localized<sup>12,13</sup>, this protein is not a definitive marker for the GMC cell type. Thus, *lgl pins* brains contain large numbers of ectopic, proliferating, self-renewing neuroblasts. Combining these *lgl pins* and *lgl pins* mutant data enables us to conclude that *Lgl* inhibits self-renewal, whereas *Pins* has dual functions in promoting and inhibiting self-renewal.

To understand how *Lgl* and *Pins* regulate neuroblast self-renewal at the cellular level, we assayed cortical polarity marker localization in mitotic larval neuroblasts. In wild-type larval neuroblasts, the Par complex (Bazooka–Par6–aPKC) and *Pins*–*Gai* proteins formed an apical crescent at metaphase and were partitioned into the self-renewing neuroblast at telophase, whereas the *Miranda* and *Prospero* proteins formed a basal crescent at metaphase and were partitioned into the differentiating GMC at telophase<sup>1</sup> (Fig. 3a, see legend). In *lgl pins* double mutants, in which all neuroblasts divided symmetrically to generate self-renewing neuroblast/neuroblast siblings, most mitotic neuroblasts showed uniform cortical aPKC, cytoplasmic Bazooka and Par6, and uniform cortical *Miranda* at metaphase and telophase (Fig. 3b, see legend). Thus, only aPKC maintained its correct subcellular localization and correlated with neuroblast self-renewal.

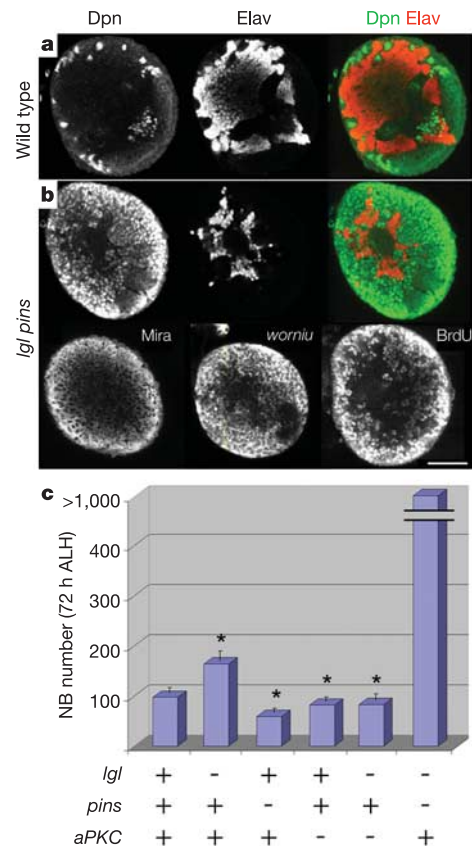


**Figure 2 | *lgl pins* double mutants have ectopic neuroblasts and fewer neurons.** **a, b**, Wild-type (**a**) and *lgl*<sup>334</sup> *pins*<sup>62</sup> (**b**) brains at 96 h ALH stained for the neuroblast markers *Deadpan*, *Miranda* and *worniu* mRNA, for BrdU incorporation, and for the neuron marker *Elav*. **c**, Quantification of *lgl*<sup>334</sup>, *pins*<sup>62</sup>, and *aPKC*<sup>K06403</sup> single- and double-mutant phenotypes in brains at 72 h ALH (+, wild type at locus; -, homozygous mutant at locus). Asterisks indicate a statistically significant difference in neuroblast number as compared with wild type ( $P \leq 2 \times 10^{-4}$ ; Student's *t*-test). Scale bar, 50  $\mu$ m.

We next examined aPKC localization in *lgl* and *pins* single mutants, in which symmetric divisions occurred at lower frequency. In *lgl* mutants, aPKC showed weak ectopic cortical localization in about half the metaphase neuroblasts, whereas Miranda was delocalized from the cortex; by telophase, however, both proteins appeared to be localized normally<sup>7,8</sup> (Fig. 3c, see legend). Ectopic cortical aPKC was also observed in *dlg* mutant larval neuroblasts (data not shown). A role for Lgl in restricting aPKC to the apical cortex of neuroblasts has not been reported<sup>7,8</sup> but would be consistent with the observation that basolateral Lgl restricts aPKC to the apical surface of *Drosophila* and vertebrate epithelia<sup>14–16</sup> and *Xenopus* blastomeres<sup>17</sup>. In *pins* mutants, aPKC and cytoplasmic Miranda showed weak uniform cortical in metaphase neuroblasts, but were properly localized in most telophase neuroblasts (Fig. 3d, see legend). Thus, both Lgl and Pins are required to restrict aPKC to the apical cortex in metaphase neuroblasts.

We next tested whether aPKC is required for neuroblast self-

renewal. *aPKC* mutant clones in larval mushroom body neuroblasts showed premature lineage termination<sup>18</sup>, consistent with aPKC being required for neuroblast self-renewal. In addition, *aPKC* null mutants died as second instar larvae with reduced neuroblast numbers (Fig. 2c). Because this was a relatively mild phenotype and there was no detectable aPKC protein at this stage, it is likely that there are additional pathways for stimulating neuroblast self-renewal. We next tested whether aPKC is required for ectopic neuroblast self-renewal in the *lgl* mutants. *lgl aPKC* double mutants had normal numbers of neuroblasts (Fig. 2c), showing that aPKC is required for the ectopic neuroblast self-renewal seen in *lgl* mutants. *aPKC* mutants also suppressed ectopic neuroblast self-renewal in several independently isolated *lgl* mutations, further supporting a role for aPKC in self-renewal (Supplementary Fig. 4). In addition, we found that *aPKC* is fully epistatic to *lgl* in regulating Miranda localization (Fig. 3c, e, f). Thus, aPKC is required for the ectopic neuroblast self-renewal and Miranda delocalization phenotypes seen in *lgl* mutants.

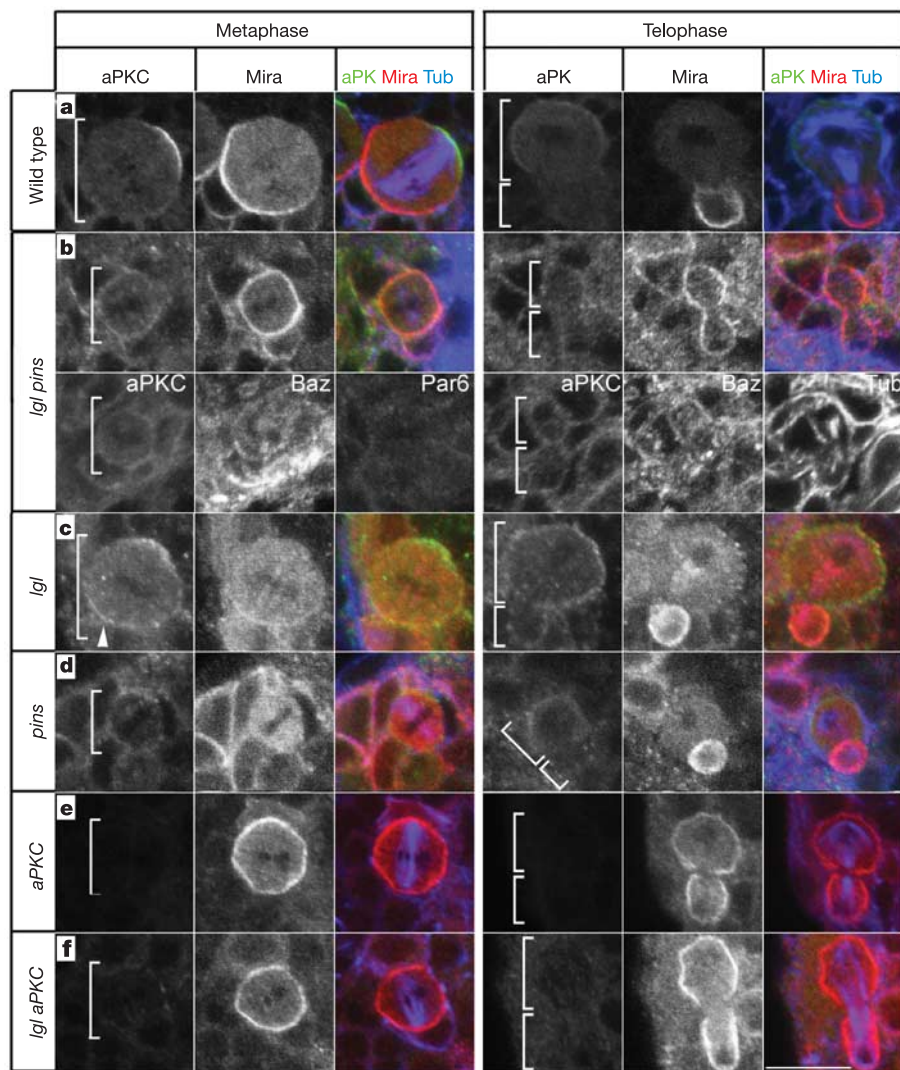


**Figure 3 | Lgl and Pins regulate aPKC localization in larval neuroblasts.** **a–f**, Brains at 72 h ALH triple-labelled with the indicated markers. Brackets indicate neuroblasts or GMCs; arrowhead indicates ectopic aPKC. **a**, Wild type. aPKC and Miranda form cortical crescents (100%; metaphase,  $n = 139$ ; telophase,  $n = 103$ ). **b**, *lgl<sup>334</sup> pins<sup>62</sup>* double mutants. At metaphase, aPKC shows ectopic cortical localization (56%;  $n = 61$ ) and Miranda is cortical or cytoplasmic. At telophase, aPKC is cytoplasmic, Miranda is uniform cortical (100% for both;  $n = 16$ ), and Bazooka and Par6 are cytoplasmic. **c**, *lgl<sup>334</sup>* mutants. At metaphase, aPKC shows weak ectopic

cortical localization (44%;  $n = 93$ ) and Miranda is delocalized (93%;  $n = 93$ ). At telophase, both are localized normally (100%;  $n = 122$ ). **d**, *pins<sup>62</sup>* mutants. At metaphase aPKC is uniform cortical and Miranda is cytoplasmic (92% for both;  $n = 92$ ), but by telophase aPKC is apical and Miranda is basal (90% for both;  $n = 30$ ). **e**, *aPKC<sup>k06403</sup>* mutants. aPKC is undetectable and Miranda is cortical from metaphase to telophase. **f**, *lgl<sup>334</sup> aPKC<sup>k06403</sup>* double mutants. aPKC is undetectable and Miranda is cortical from metaphase to telophase (100%  $n = 36$ ). Scale bar, 10  $\mu$ m.

Our data are most consistent with a model in which Lgl negatively regulates aPKC, and aPKC directly promotes self-renewal. This model is based on the observations that Lgl restricts aPKC localization to the apical cortex of neuroblasts and that a reduction in aPKC blocks the *lgl* self-renewal phenotype. To test this model, we used *worniu-Gal4* line to drive neuroblast-specific expression of constitutively active aPKC or Lgl proteins, and assayed for an increase or decrease in neuroblast numbers. Neuroblast-specific expression of aPKC targeted to the plasma membrane with a CAAX prenylation motif (*UAS-aPKC<sup>CAAXWT</sup>*)<sup>19</sup> resulted in ectopic cortical aPKC localization, loss of cortical Miranda (Fig. 4a), and a large increase in the number of neuroblasts (Fig. 4g, j, and Supplementary Movie 5). These effects were not observed after overexpression of wild-type aPKC<sup>10</sup> or a membrane-targeted kinase-dead aPKC (*UAS-aPKC<sup>CAAXKD</sup>*)<sup>19</sup> (Fig. 4b, d, h, j, and Supplementary Movie 6). Expression of a constitutively active aPKC (*UAS-aPKC<sup>ΔN</sup>*)<sup>10</sup> that was predominantly cytoplasmic (Fig. 4c) gave only a slight increase in neuroblast number (Fig. 4j), showing that cortical localization of aPKC is essential to generate ectopic neuroblasts. By contrast, neuroblast-specific expression of a constitutively active Lgl protein (Lgl3A) resulted in the expected uniform cortical localization of Miranda (Fig. 4e)<sup>10</sup>, but no change in neuroblast numbers (Fig. 4j). Combined overexpression of both Lgl3A and aPKC<sup>CAAXWT</sup>, however, resulted in strong suppression of the aPKC<sup>CAAXWT</sup> ectopic neuroblast phenotype (Fig. 4i, j), even though Lgl3A alone had no effect on

neuroblast numbers, consistent with Lgl inhibiting aPKC function either directly or at through its downstream effectors. Thus, neuroblast-specific overexpression of aPKC can expand the neuroblast population (most probably by promoting symmetric neuroblast/neuroblast cell divisions) without eliminating the ability of these neuroblasts to undergo asymmetric neuroblast/GMC divisions to generate differentiating progeny. We conclude that aPKC is sufficient to promote neuroblast self-renewal, Lgl can inhibit aPKC function, and membrane-targeting and kinase activity are essential for aPKC function.

We have established *Drosophila* larval neuroblasts as a model system for studying self-renewal versus differentiation. We have proposed a simple model in which Pins anchors aPKC apically and Lgl inhibits aPKC localization basally, thereby restricting aPKC to the apical cortex where it promotes neuroblast self-renewal (Fig. 4k). In addition, aPKC can phosphorylate and directly inhibit Lgl function<sup>10</sup>, which together with our data provides evidence for mutual inhibition between Lgl and aPKC in neuroblasts, similar to the mutual inhibition seen between these two proteins in epithelia<sup>14–17</sup>. Mutual inhibition between aPKC and Lgl would result in stabilization of apical aPKC localization and more reliable partitioning of aPKC into the neuroblast during mitosis. In *pins* mutants, aPKC is delocalized and nonfunctional owing to Lgl activity, thereby reducing self-renewal; in *lgl* mutants, aPKC shows weak ectopic cortical localization that increases self-renewal; and in *lgl pins* double mutants, aPKC is both delocalized and fully active, and thus all neuroblasts undergo symmetric self-renewal (Fig. 4k). Although the targets of aPKC involved in self-renewal are unknown, aPKC may directly phosphorylate and inactivate GMC determinants<sup>20</sup>, and/or phosphorylate and activate neuroblast-specific proteins. Notably, *lgl* mutant mice have neural progenitor hypertrophy<sup>21</sup> and knockdown of a *pins* mammalian homologue (AGS3) leads to depletion of neural progenitors<sup>22</sup>; phenotypes that are very similar to those described here. In the future, it will be important to determine the role of aPKC in mammalian neural progenitor self-renewal and to identify the aPKC-regulated phosphoproteins that regulate neuroblast self-renewal in *Drosophila*.

## METHODS

All fly stocks have been described<sup>10,11,18,19,23,24</sup>. Neuroblast clones were generated as described<sup>25</sup> using a 90-min heat shock at 37 °C to larvae at 24 h ALH with recovery at 25 °C. Published methods were used for BrdU pulse labelling<sup>4</sup>, *worniu* ribonucleotide probe generation<sup>26</sup>, fluorescent *in situ* hybridization<sup>27</sup> and antibody staining<sup>18</sup> (details are available on request from the authors and in the Supplementary Methods).

Received 27 July; accepted 3 October 2005.  
Published online 14 December 2005.

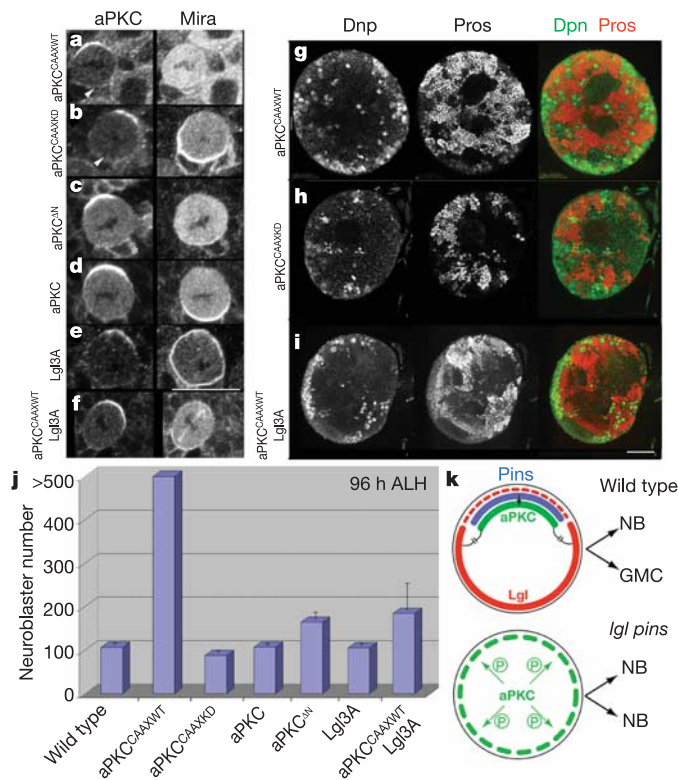


**Figure 4 | Overexpression of cortical aPKC promotes neuroblast self-renewal.** **a–i**, Expression of the indicated *UAS* transgenes (left) by *worniu-Gal4* in brains at 96 h ALH stained for the indicated markers (top). All neuroblasts expressed the correct molecular markers (Deadpan<sup>+</sup>, nuclear-Prospero<sup>+</sup>), were proliferative (BrdU<sup>+</sup>) and could even generate smaller nuclear-Prospero<sup>+</sup> GMCs (**g–i**; data not shown). Scale bars, 10 μm (**a–f**); 50 μm (**g–i**). Arrowheads indicate ectopic aPKC; asterisks indicate aPKC<sup>+</sup> GMCs contacting neuroblast. **j**, Quantification of neuroblast number (Student *t*-test). Wild type, 98.9 ± 4.6; aPKC<sup>CAAXWT</sup>, >500; aPKC<sup>CAAXKD</sup>, 87.4 ± 4.6; aPKC, 99.5 ± 3; aPKC<sup>ΔN</sup>, 150.4 ± 15.7; Lgl3A, 97.6 ± 4.4; aPKC<sup>CAAXWT</sup> Lgl3A, 173.6 ± 61.7 (means ± s.d.). **k**, Model of the role of Pins, Lgl and aPKC in regulating neuroblast self-renewal. See text for details.

- Betschinger, J. & Knoblich, J. A. Dare to be different: asymmetric cell division in *Drosophila*, *C. elegans* and vertebrates. *Curr. Biol.* **14**, R674–R685 (2004).
- Ohlstein, B., Kai, T., Decotto, E. & Spradling, A. The stem cell niche: theme and variations. *Curr. Opin. Cell Biol.* **16**, 693–699 (2004).
- Urbach, R. & Technau, G. M. Neuroblast formation and patterning during early brain development in *Drosophila*. *BioEssays* **26**, 739–751 (2004).
- Datta, S. Control of proliferation activation in quiescent neuroblasts of the *Drosophila* central nervous system. *Development* **121**, 1173–1182 (1995).
- Gateff, E. & Schneiderman, H. A. Developmental capacities of benign and malignant neoplasms of *Drosophila*. *Roux Arch. Dev. Biol.* **176**, 23–65 (1974).
- Ohshiro, T., Yagami, T., Zhang, C. & Matsuzaki, F. Role of cortical tumour-suppressor proteins in asymmetric division of *Drosophila* neuroblast. *Nature* **408**, 593–596 (2000).
- Peng, C. Y., Manning, L., Albertson, R. & Doe, C. Q. The tumour-suppressor genes *lgl* and *dlg* regulate basal protein targeting in *Drosophila* neuroblasts. *Nature* **408**, 596–600 (2000).
- Albertson, R. & Doe, C. Q. *Dlg*, *Scrib* and *Lgl* regulate neuroblast cell size and mitotic spindle asymmetry. *Nature Cell Biol.* **5**, 166–170 (2003).
- Strand, D. *et al.* The *Drosophila* lethal(2)giant larvae tumour suppressor protein forms homo-oligomers and is associated with nonmuscle myosin II heavy chain. *J. Cell Biol.* **127**, 1361–1373 (1994).
- Betschinger, J., Mechtler, K. & Knoblich, J. A. The Par complex directs asymmetric cell division by phosphorylating the cytoskeletal protein Lgl. *Nature* **422**, 326–330 (2003).

11. Buenzow, D. E. & Holmgren, R. Expression of the *Drosophila* gooseberry locus defines a subset of neuroblast lineages in the central nervous system. *Dev. Biol.* **170**, 338–349 (1995).
12. Freeman, M. R. & Doe, C. Q. Asymmetric Prospero localization is required to generate mixed neuronal/glial lineages in the *Drosophila* CNS. *Development* **128**, 4103–4112 (2001).
13. Spana, E. P. & Doe, C. Q. The Prospero transcription factor is asymmetrically localized to the cell cortex during neuroblast mitosis in *Drosophila*. *Development* **121**, 3187–3195 (1995).
14. Bilder, D., Li, M. & Perrimon, N. Cooperative regulation of cell polarity and growth by *Drosophila* tumour suppressors. *Science* **289**, 113–116 (2000).
15. Hutterer, A., Betschinger, J., Petronczki, M. & Knoblich, J. A. Sequential roles of Cdc42, Par-6, aPKC, and Lgl in the establishment of epithelial polarity during *Drosophila* embryogenesis. *Dev. Cell* **6**, 845–854 (2004).
16. Yamanaka, T. *et al.* Mammalian Lgl forms a protein complex with PAR-6 and aPKC independently of PAR-3 to regulate epithelial cell polarity. *Curr. Biol.* **13**, 734–743 (2003).
17. Chalmers, A. D. *et al.* aPKC, Crumbs3 and Lgl2 control apicobasal polarity in early vertebrate development. *Development* **132**, 977–986 (2005).
18. Rolls, M. M., Albertson, R., Shih, H. P., Lee, C. Y. & Doe, C. Q. *Drosophila* aPKC regulates cell polarity and cell proliferation in neuroblasts and epithelia. *J. Cell Biol.* **163**, 1089–1098 (2003).
19. Sotillos, S., Diaz-Meco, M. T., Caminero, E., Moscat, J. & Campuzano, S. DaPKC-dependent phosphorylation of Crumbs is required for epithelial cell polarity in *Drosophila*. *J. Cell Biol.* **166**, 549–557 (2004).
20. Caussinus, E. & Gonzalez, C. Induction of tumour growth by altered stem-cell asymmetric division in *Drosophila melanogaster*. *Nature Genet.* **37**, 1125–1129 (2005).
21. Klezovitch, O., Fernandez, T. E., Tapscott, S. J. & Vasioukhin, V. Loss of cell polarity causes severe brain dysplasia in *Lgl1* knockout mice. *Genes Dev.* **18**, 559–571 (2004).
22. Sanada, K. & Tsai, L. H. G Protein  $\beta\gamma$  subunits and AGS3 control spindle orientation and asymmetric cell fate of cerebral cortical progenitors. *Cell* **122**, 119–131 (2005).
23. Yu, F., Morin, X., Cai, Y., Yang, X. & Chia, W. Analysis of partner of inscuteable, a novel player of *Drosophila* asymmetric divisions, reveals two distinct steps in inscuteable apical localization. *Cell* **100**, 399–409 (2000).
24. Albertson, R., Chabu, C., Sheehan, A. & Doe, C. Q. Scribble protein domain mapping reveals a multistep localization mechanism and domains necessary for establishing cortical polarity. *J. Cell Sci.* **117**, 6061–6070 (2004).
25. Pearson, B. J. & Doe, C. Q. Regulation of neuroblast competence in *Drosophila*. *Nature* **425**, 624–628 (2003).
26. Freeman, M. R., Delrow, J., Kim, J., Johnson, E. & Doe, C. Q. Unwrapping glial biology: Gcm target genes regulating glial development, diversification, and function. *Neuron* **38**, 567–580 (2003).
27. Grosskortenhaus, R., Pearson, B. J., Marusich, A. & Doe, C. Q. Regulation of temporal identity transitions in *Drosophila* neuroblasts. *Dev. Cell* **8**, 193–202 (2005).

**Supplementary Information** is linked to the online version of the paper at [www.nature.com/nature](http://www.nature.com/nature).

**Acknowledgements** We thank J. Knoblich, S. Campuzano, B. Chia, J. Skeath and B. Holmgren for fly stocks and/or antibody reagents; B. Bowerman, J. Eisen, K. Siller and S. Siegrist for comments on the manuscript; and C. Chabu for discussion. C.-Y.L. is supported by a Damon Runyon postdoctoral fellowship. C.Q.D. is supported by the Howard Hughes Medical Institute, where he is an Investigator.

**Author Information** Reprints and permissions information is available at [npg.nature.com/reprintsandpermissions](http://npg.nature.com/reprintsandpermissions). The authors declare no competing financial interests. Correspondence and requests for materials should be addressed to C.Q.D. ([cdoe@uoregon.edu](mailto:cdoe@uoregon.edu)).